PRELIMINARY NUMERICAL AND EXPERIMENTAL ANALYSIS OF THE SPALLATION PHENOMENON

Alexandre Martin[*1], **Sean C.C. Bailey**[†1], **Francesco Panerai**[‡1,2], **Raghava S.C. Davuluri**[§1], **Alexander R. Vazsonyi**[¶1], **Huaibao Zhang**[§1], **Zachary S. Lippay**[¶1], **Nagi N. Mansour**[‖2], **Jennifer A. Inman**[**3], **Brett F. Bathel**[**3], **Scott C. Splinter**[††3], **and Paul M. Danehy**[**3]

[1]*University of Kentucky, Lexington, KY 40506*
[2]*NASA Ames Research Center, Moffett Field, CA, 94035*
[3]*NASA Langley Research Center, Hampton, VA, 23681*

ABSTRACT

The spallation phenomenon was studied through numerical analysis using a coupled Lagrangian particle tracking code and a hypersonic aerothermodynamics computational fluid dynamics solver. The results show that carbon emission from spalled particles results in a significant modification of the gas composition of the post-shock layer. Preliminary results from a test-campaign at the NASA Langley HYMETS facility are presented. Using an automated image processing of high-speed images, two-dimensional velocity vectors of the spalled particles were calculated. In a 30 second test at 100 W/cm^2 of cold-wall heat-flux, more than 1300 particles were detected, with an average velocity of 102 m/s, and most frequent observed velocity of 60 m/s.

Key words: ablation; spallation; arc-jet; thermal protection system.

1. INTRODUCTION

Low density ablators are one of the preferred class of material for protecting space vehicles during atmospheric entry. Through various physical processes [7, 14] such as near-surface oxidation, pyrolysis chemical reaction, vaporization, and other decomposition processes, these materials reduce the amount of heat being conducted to the surface of the vehicle. These beneficial processes usually fall under the umbrella term "ablation". The spallation phenomenon [6, 11] also belongs in this category; however, unlike the other processes involved in ablation, spallation is generally regarded as undesirable.

[*]Assistant Professor, Department of Mechanical Engineering, alexandre.martin@uky.edu
[†]Assistant Professor, Department of Mechanical Engineering
[‡]Research Fellow, Department of Mechanical Engineering, NASA Visiting Scientist, Thermal Protection, Materials Branch
[§]Graduate Student, Department of Mechanical Engineering
[¶]Student, Department of Mechanical Engineering
[‖]Chief Scientist, Advanced Supercomputing Division
[**]Research Scientist, Advanced Measurements and Data Systems Branch
[††]Aerospace Engineer, Structural Mechanics and Concepts Branch

Spallation is typically described as the ejection of solid particles off the surface of the material. Those particle are then convected away in the flow field. The exact cause of this phenomenon is unclear, although it is likely to be caused by mechanical erosion of the fibrous surface, and weakened by oxidative decomposition, combined with the shear stresses introduced by the fluid flow. Soot formation from the pyrolysis gas is also a potential cause of spalled particles.

The aerodynamic heating rates of re-entry vehicles may be affected by spallation through various mechanisms. For instance, the solid particles ejected from the surface can modify the near surface chemical processes and flow field. Mechanical erosion can lead to an irregular surface, and in turn, to an augmented surface roughness. Such a modification of the surface, as well as the presence of particles in the boundary layer, could potentially trigger transition from laminar to turbulent flow. Finally, mechanical erosion results in an accelerated surface recession, thereby reducing the effectiveness of the thermal protection system (TPS). Material response codes, such as the ones used by NASA to design TPS, take into account this accelerated failure mechanism through introduction of an empirically calculated parameter [8]. Therefore, there is a need to better understand and model the spallation phenomenon, including its source and impact on TPS performance.

To further investigate spallation effects, a Lagrangian particle tracking code was developed. This code computes the dynamics of spalled particles as they travel through a flow field. The code uses a finite-rate chemistry model to predict the chemical interactions of the particles with the flow field. This particle tracking code can then be dynamically coupled to a computational fluid dynamics (CFD) solver which models the time-accurate hypersonic flow field around ablative samples. A preliminary analysis performed using this coupled approach is presented here.

To support the spallation modeling effort, an experimental investigation was performed at the NASA Langley Hypersonic Materials Environmental Test System (HYMETS) facility [4]. HYMETS is a 400 kW arcjet

that can simulate hypersonic flight and Earth or Martian entry conditions. High speed imagery was used to capture spalled particles ejecting from FiberForm®, and PICA test samples at target heat flux conditions of 100, 200, and 400 W/cm^2. From this data, measurements of particle velocity and trajectory were obtained. An initial assessment of the data for one FiberForm® sample is presented here.

2. NUMERICAL SIMULATIONS

2.1. Numerical models

The flow field solutions used to predict the trajectories of spalled particles following ejection from the surface were obtained using the hypersonic CFD code KATS – Kentucky Aerothermodynamics and Thermal-response Solver [16, 17]. KATS is a three-dimensional laminar Navier-Stokes solver that computes flow fields in thermochemical non-equilibrium in the continuum regime. The translational and rotational energy modes of the species of the gas are described by a single temperature T_{tr}, while the vibrational and electronic energy modes, as well as electron translational energy mode, are characterized by another single temperature T_{ve}. The individual species viscosity model used to compute the diffusive fluxes was obtained using the Blottner curve fits [1]. Euken's relations [13] were used to account for species thermal conductivity. The mixture transport properties are approximated using Wilke's semi-empirical mixing rule. For reacting flows, a standard finite-rate chemical kinetics model was used.

The spallation code used for this preliminary analysis models the dynamics of individual particles ejected from the surface of a test articles, using a steady-state flow-field solution as an initial condition. The code uses the flow field information to determine the trajectory of the particle. The following assumptions are used to derive the governing equations:

1. The spalled particles are spherical
2. The spalled particles are made of graphite
3. Heat and mass transfer rates are uniform over the surface of the particle
4. Thermophysical properties of the particle are assumed to be uniform over the entire particle

Graphite is chosen since charred PICA is considered to be carbon, and that thermochemical properties of graphite are available in the literature. A Lagrangian formulation is employed to compute the projected path of the spalled particle. The corresponding governing equations are

$$\frac{\partial}{\partial t}\begin{pmatrix} m_p \\ m_p \mathbf{u_p} \\ m_p E_p \end{pmatrix} = \begin{pmatrix} -\dot{m}_{\mathrm{C/CO}} - \dot{m}_{\mathrm{C/CN}} - \dot{m}_{C/sub} \\ \mathbf{F_D} \\ \dot{q}_{conv} + p_{drag} - \dot{q}_{rad} + \dot{q}_{rxn} \end{pmatrix}. \tag{1}$$

In the left hand side, m_p, $\mathbf{u}_p$ and E_p are respectively the mass, the velocity vector and the energy of the spalled particle. In the right hand side, $\mathbf{F_D}$, $\dot{q}_{conv}$, p_{drag}, $\dot{q}_{rad}$ and $\dot{q}_{rxn}$ are, respectively, the drag force, the convective heating, the power loss caused by drag, the re-radiative heating and the chemical energy term.

Table 1. Surface chemistry model used to calculate the erosion of the spalled particles in the flow field

Reactions	Type
$\mathrm{C(s) + O \longrightarrow CO}$	Oxidation
$\mathrm{2\,C(s) + O_2 \longrightarrow 2\,CO}$	Oxidation
$\mathrm{C(s) + N \longrightarrow CN}$	Nitridation
$\mathrm{C(s) \longrightarrow C}$	Sublimation
$\mathrm{2\,C(s) \longrightarrow C_2}$	Sublimation
$\mathrm{3\,C(s) \longrightarrow C_3}$	Sublimation

Table 2. Free stream and wall properties of the Mach 5 argon flow

ρ_∞ [kg/m^3]	U_∞ [m/s]	T_{tr} [K]	T_{ve} [K]	T_w [K]
3.45×10^{-3}	3860	1470	1470	500

As they travel in the flow field, the particles chemically react with the flow. As the particles lose mass, their radius is reduced. The gas/particle interaction is modeled using a finite-rate rate chemistry model that accounts for three types of non-homogeneous reactions: oxidation, nitridation, and sublimation [3]. The three types are respectively represented in Eq. 1 by the mass source terms $\dot{m}_{\mathrm{C/CO}}$, $\dot{m}_{\mathrm{C/CN}}$ and $\dot{m}_{C/sub}$. The complete reaction mechanism is provided in Table 1.

This spallation model and coupling strategy has been extensively verified; more details are given in Ref. [3]

2.2. Preliminary results

The test case considered here consists of a Mach 5 high enthalpy flow over an axi-symmetric solid sample with a radius of 3.30 cm, and an axial length of 0.82 cm. These test conditions are representative of what is observed in the HYMETS facility [2, 4].

First, a parametric study was performed to evaluate the effects of the ejection conditions (ejection velocity, particle size and ejection angle) on the trajectory of the particle [3]. For the flow field, a Mach 5 argon flow was used, with flow conditions listed in Table 2. In the table, T_w refers to the temperature at the surface of the sample. Argon was chosen as it simplifies the flow field solution, and allow the particle to travel the flow field without reacting. As can be seen in Fig. 1(a) to Fig. 1(c), changing the ejection conditions considerably changes the trajectory of the particle. Therefore, if trajectories are measured experimentally, they could provide valuable insights about the ejection conditions.

Next, to allow evaluation of the effects of a spalled particle interacting with a flow field upstream of a test arti-

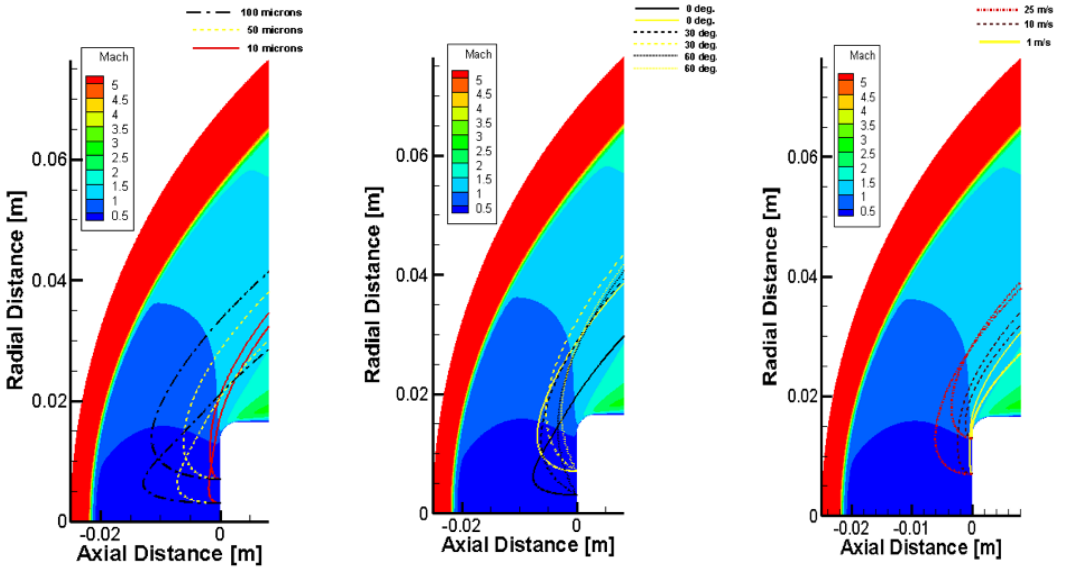

(a) Particle radius variation ($v_p = 25$ m/s, $\theta = 0°$)

(b) Angle variation ($m_p = 10$ µm, $v_p = 100$ m/s)

(c) Ejection velocity variation ($m_p = 50$ µm, $\theta = 0°$)

Figure 1. Particle trajectories as a result of the study for the ejection parameters of spalled particle in a Mach 5 argon flow

cle, the spallation code was coupled with KATS. Using a time-accurate simulation, the carbon species emitted by the spalled particle traveling in the flow field was transferred to the CFD code through mass source terms. For this specific case, a Mach 5 air flow field is used, with conditions listed in Table 3. In this table, Y_i represents the mass faction of individual species i. For this simulation, a 30 micron carbon particle was ejected normal to the surface, 5 mm from the stagnation point, at a velocity of 90 m/s. The simulation takes place over a physical time of 0.7 ms, and the results are presented in Fig. 2. In Fig. 2(a), the entire trajectory of the particle is seen over the temperature field. It can be seen in Fig. 2(b) to Fig. 2(d) that the particle ejects a significant amount of carbon species, and that this carbon diffuses around the particles in all directions before being convected away. It is clear from this preliminary analysis that these carbon species would react with the incoming flow, and that additional species such as CN could be created. These observations reinforce the hypothesis that spalled particles could be responsible for a previously unexplained strong spectroscopic signature observed in some arc-jet test data upstream of the sample [5, 9, 10, 15].

3. EXPERIMENT

3.1. Facility and instrumentation

A series of preliminary test was performed at the HYMETS facility at the NASA Langley Research Center to assess the feasibility of identifying and tracking spalled particles ejected from TPS materials. As opposed to large-scale arc-jet wind tunnels, HYMETS can be operated by a minimal staff, can be run for a long period, and has essentially no downtime between runs. Hence, it is ideal for exploratory studies such as those of the present research effort. Moreover, the facility is equipped with numerous optical ports which allow the possibility of complex diagnostics and image capturing [4].

As previously noted, the purpose of the present test-campaign was to confirm the presence of spalled particles for different test articles throughout a range of flow conditions. During these tests, the facility was equipped with the following:

- four high speed cameras for particle detection at different view angles, two of them linked for stereoscopic measurements
- two spectrometers (VUV and N-IR)
- an infrared camera
- a two color single-point pyrometer for surface temperature measurements
- three intrusive probes for flow calibration
- three thermocouples at the back face of each sample

A total of ten samples of PICA [12] and FiberForm® were tested in air plasma, under three cold-wall heat flux conditions (100, 200 and 400 W/cm^2). All samples had a diameter of 3.30 cm, and a height of 2.54 cm, which included a 0.38 cm Li-2200 collar for some samples. In addition, three graphite, and three Li-2200 samples were tested under the same heat fluxes. The following section present preliminary measurements on spalling particle with high speed imaging, leaving a thorough documentation of the test campaign measurements to future publications.

Fig. 3 is a composite image compiled from all frames during a 30 s test of FiberForm® at 100 W/cm^2. The images

Table 3. Free stream temperature and wall properties of the Mach 5 air flow

ρ_∞ [kg/m^3]	U_∞ [m/s]	T_{tr} [K]	T_{ve} [K]	T_w [K]	Y_{Ar}	Y_{N_2}	Y_{O_2}	Y_{NO}	Y_N	Y_O
1.46×10^{-3}	3163	896	896	600	0.0704	0.7178	0.0613	0.0469	0.0000	0.1036

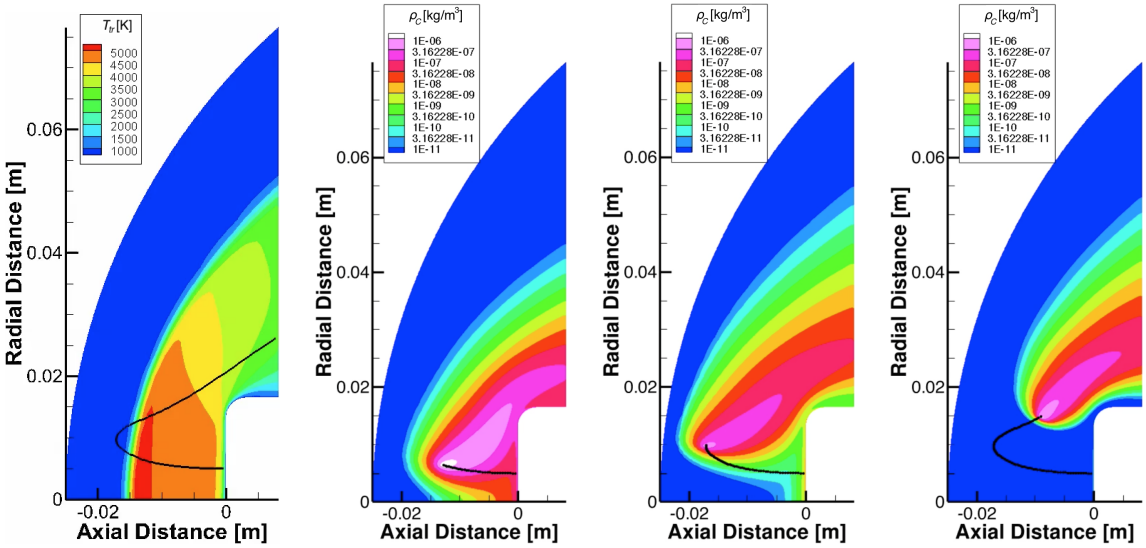

(a) Trajectory and temperature field

(b) Carbon density, t =0.17 ms

(c) Carbon density, t =0.35 ms

(d) Carbon density, t =0.53 ms

Figure 2. Temperature field, trajectory and density of the carbon species emitted from a 30 micron spalled particle ejected at 90 m/s in a Mach 5 air flow.

used to construct this figure were obtained using a 12-bit monochrome pco.dimax HD high-speed CMOS camera, cropped down to 672×608 pixels from the 1920×1080 full sensor array in order to reduce file size. As can be seen, numerous spalled particles are observed being ejected from the samples. The same observation was made at flows with lower cold-wall heat flux conditions. Spallation was systematically observed during all tests of FiberForm® and PICA samples. The graphite and Li-2200 samples however, showed no evidence of spallation.

3.2. Particle tracking

To provide a quantitative evaluation of the spalled particle behavior, data was analyzed from an IDT MotionXtra N-4S1, 1016×1016, 10-bit mono camera located orthogonally to the sample. The test case presented here is for a FiberForm® sample subjected to a 200 W/cm^2 heat flux for 30 s. The camera was set to double-exposure mode with the first exposure of 30 µs, followed 100 ns later by a second exposure of approximately 470 µs. Due to limitations in the on-board memory of the camera, both exposures were acquired at a sampling frequency of only 15 Hz. This ensured that images were acquired for the entire duration of the 30 s placement of the sample within the arc-jet. As a result, 946 images were acquired over 31.5 s, with 473 images acquired at each exposure duration.

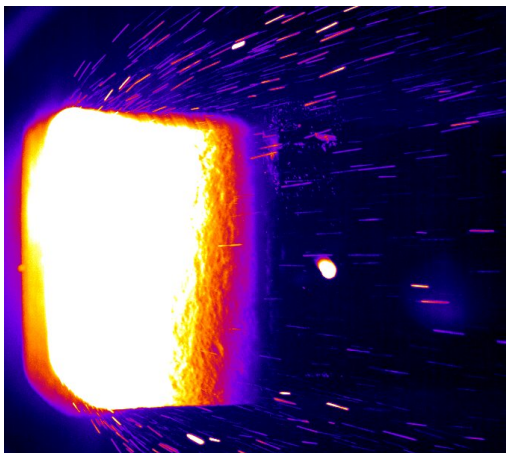

Figure 3. Integrated image of a FiberForm® samples subjected to a 400 W/cm^2 heat flux. The image is a reconstruction formed by combining the brightest pixel of approximately 900 images taken during a 30-second experiment. These images were acquired at a frame rate of 30 Hz with an exposure time of 25 µs

It should be note that only the first exposure was analyzed, with analysis of the second exposure left for future work. A single, unprocessed image is shown in Fig. 4(a). A small particle trace can be seen in the top of the im-

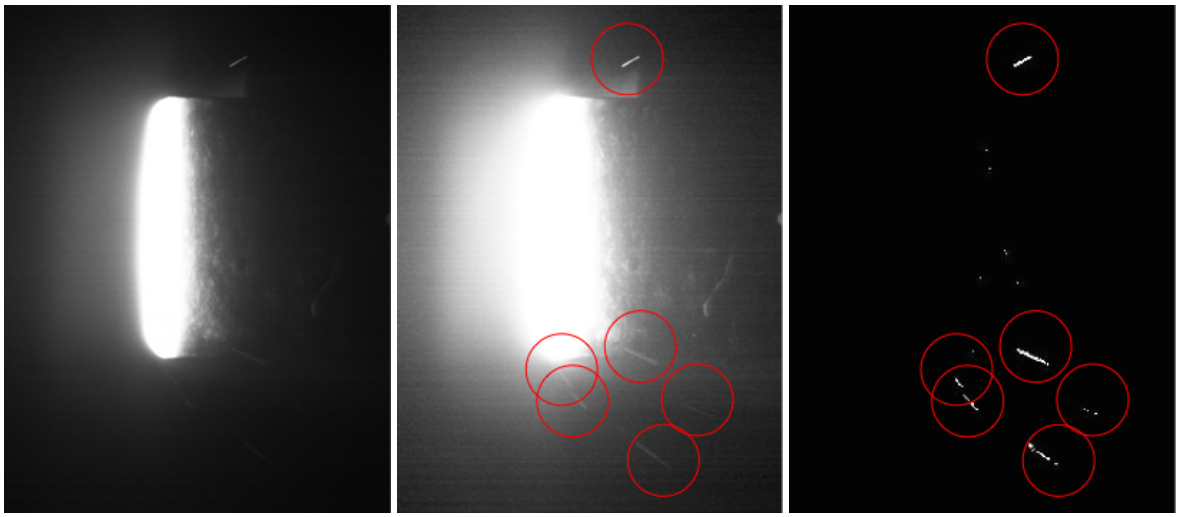

(a) Original image (b) Enhanced image (c) Processed image

Figure 4. FiberForm® sample subjected to a 200 W/cm^2 heat flux; after processing the image, six spalled particles are identified.

age, and shadows of others at the bottom. However, by re-scaling the pixel intensities, as done in Fig. 4(b), multiple spalled particles are clearly observed, with five being identified in this single 30 μs exposure.

To analyze the image, a processing scheme was developed to isolate and enhance the particles. The first step in this process consists of subtracting the background information obtained by averaging the five consecutive images centered on the image of interest. This subtraction did not completely remove all of the radiated light emitted from the front of the sample, and therefore pixels within this region were discarded. Next, using a pixel intensity threshold, the remaining pixels were identified and flagged as belonging to spalled particles. Finally, an algorithm was implemented which identified groups of neighboring pixels within a 6×6 pixel moving window were identified and each separate group marked as a "spalled particle". Groups containing ten or fewer pixels were identified as "false positives". This process was fully automated using MATLAB®. The result is shown in Fig. 4(c).

Using this process, more than 1300 particles were identified over the 400 images obtained during a single run. By using the exposure length and the pixel grouping geometry, two-dimensional velocity vectors in the plane of the camera can be estimated. A compilation of the velocity vectors detected during the run is presented in Fig. 5. With this approach, the velocities are projected in the plane captured by the camera, and they are thus subjected to a two-dimensional approximation. As expected, the velocity around the centerline of the sample appear to be smaller since the velocity components in the z direction is not measured.

From these results it is also possible to evaluate the normalized distribution of velocity for all the spalled particles that were identified. Fig. 6 plots the distribution

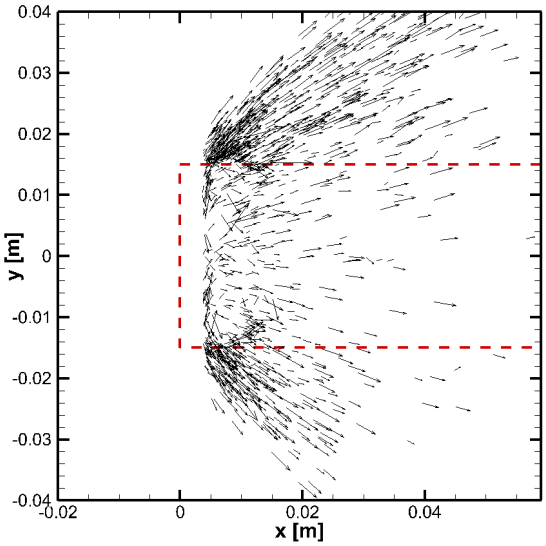

Figure 5. Two-dimensional velocity vectors (in the camera plane) of the detected spalled particles estimated by exposure length and pixel grouping geometry. Red line shows the location of the test article.

of the particle with respect to their calculated xy-plane velocity. The probability is calculated by counting the number of particles which have a velocity within a certain range, and then normalizing over the total number of particles. The average velocity component of particles in the two-dimensional image plane was estimated to be 102 m/s, However the distribution of the particle velocity was highly skewed, with the most frequent (probable) velocity closer to 60 m/s.

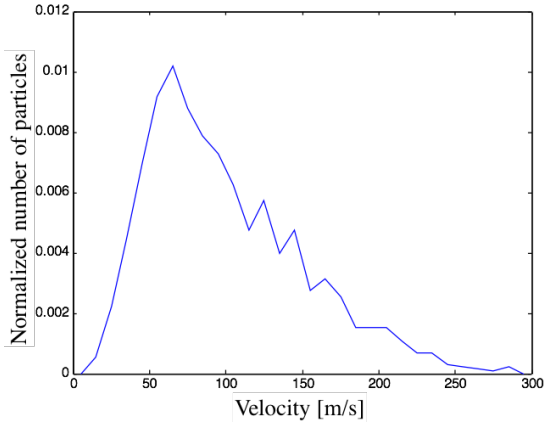

Figure 6. Magnitude of the velocity distribution of the detected spalled particles. The magnitude is only calculated using two measured components, in the camera plane.

4. CONCLUSION AND OUTLOOK

This paper presents the recent advances in research related to the ablative phenomenon – spallation. To investigate the effects of spallation on the flow field, a numerical code was developed. The results showed that a spalled particle ejected in a reacting flow would release carbon species in the flow field. This carbon is in sufficient quantity that it is likely to form CN species, and therefore explain the CN emission detected by spectroscopic experiments.

High speed imaging measurements allowed observation of multiple spalled particles during an arc-jet test run on PICA and FiberForm® samples. An automated image analysis procedure allowed detection of as many as 1300 single particles being ejected from the surface during a 30 s test run.

These results, although still preliminary, are very encouraging. Particle tracking based on stereoscopic imaging will enable improvements in the determination of particle velocities and trajectories in the three-dimensional space. Using the numerical method combined with the images obtained during the test campaign, it will be possible to gather more information about the trajectory and initial state of the spalled particles. This will undoubtedly lead to a better understanding on how these particles are formed, and what process is responsible for their high-speed ejection.

ACKNOWLEDGMENTS

Financial support for this work was provided by NASA Kentucky EPSCoR Award NNX10AV39A and NASA Award NNX13AN04A. Additional support was generously provided by the Hypersonic EDL program, through M.J. Wright at NASA Ames. The authors are immensely grateful to him. They also would like to thank M.J. Gasch at NASA Ames, and J.G. Gragg and S.B. Jones at NASA Langley for their technical assistance. Lastly, the author are grateful to K.A. Tagavi for carefully reviewing the manuscript, as well as E. Sozer at NASA Ames Research Center for numerous insightful discussions on the CFD code.

REFERENCES

[1] Blottner, F. G., Johnson, M., & Ellis, M. 1971, Chemically reacting viscous flow program for multi-component gas mixtures., Tech. Rep. SC-RR-70-754, Sandia National Laboratories, Albuquerque, New Mexico

[2] Danehy, P. M., Hires, D. V., Johansen, C. T., Bathel, B. F., Jones, S. B., Gragg, J. G., Splinter, S. C. 2012, in 50th AIAA Aerospace Sciences Meeting and Exhibit, AIAA Paper 2012-856, Nashville, TN

[3] Davuluri, R. S. C., Zhang, H., & Martin, A. 2015, Journal of Thermophysics and Heat Transfer, 29

[4] Inman, J. A., Bathel, B. F., Johansen, C. T., Danehy, P. M., Jones, S. B., Gragg, J. G., Splinter, S. C. 2013, AIAA Journal, 51, 2365

[5] Kihara, H., Hatano, M., Nakiyama, N., Abe, K., & Nishida, M. 2006, Transactions of the Japan Society for Aeronautical and Space Sciences, 49, 65

[6] Lundell, J. H. 1982, in AIAA/ASME 3rd Joint Thermophysics and Heat Transfer Conference, AIAA Paper 82-0852, St. Louis, MO

[7] Martin, A. & Boyd, I. D. 2015, Journal of Thermophysics and Heat Transfer, 29, in Press

[8] Milos, F. & Chen, Y.-K. 2010, in 10th AIAA/ASME Joint Thermophysics and Heat Transfer Conference, AIAA Paper 2010-4663, Chicago, IL

[9] Park, C., Raiche, G. A., & Driver, D. M. 2004, Journal of Thermophysics and Heat Transfer, 18, 519

[10] Raiche, G. A. & Driver, D. M. 2004, in 42th AIAA Aerospace Sciences Meeting and Exhibit, AIAA Paper 2004-0825, Reno NV

[11] Sullivan, J. M. & Kobayashi, W. S. 1987, in 22nd AIAA Thermophysics Conference, AIAA Paper 1987-1516, 1–7

[12] Tran, H. K., Johnson, C. E., Rasky, D. J., Hui, F. C. L., Hsu, M.-T., Chen, Y. K. 1996, in 31st AIAA Thermophysics Conference, AIAA Paper 1996-1911, New Orleans, LA, 1–14

[13] Vincenti, W. G. & Kruger, C. H. 1982, Introduction to Physical Gas Dynamics (Krieger Publishing Company)

[14] Weng, H., Bailey, S. C. C., & Martin, A. 2015, International Journal of Heat and Mass Transfer, 80, 570

[15] Yoshinaka, T. 1998, Spallation Measurement at the Ablator Plasma Wind Tunnel Tests, Tech. Rep. NASDA-TMR-970006E, National Space Development Agency of Japan, Tokyo

[16] Zhang, H., Martin, A., & McDonough, J. M. 2012, in 24th International Conference on Parallel Computational Fluid Dynamics, Atlanta, GA

[17] Zhang, H., Weng, H., & Martin, A. 2014, in 52nd AIAA Aerospace Sciences Meeting, AIAA Paper 2014-1209, National Harbor, MD